



저작자표시-비영리-변경금지 2.0 대한민국

이용자는 아래의 조건을 따르는 경우에 한하여 자유롭게

- 이 저작물을 복제, 배포, 전송, 전시, 공연 및 방송할 수 있습니다.

다음과 같은 조건을 따라야 합니다:



저작자표시. 귀하는 원저작자를 표시하여야 합니다.



비영리. 귀하는 이 저작물을 영리 목적으로 이용할 수 없습니다.



변경금지. 귀하는 이 저작물을 개작, 변형 또는 가공할 수 없습니다.

- 귀하는, 이 저작물의 재이용이나 배포의 경우, 이 저작물에 적용된 이용허락조건을 명확하게 나타내어야 합니다.
- 저작권자로부터 별도의 허가를 받으면 이러한 조건들은 적용되지 않습니다.

저작권법에 따른 이용자의 권리는 위의 내용에 의하여 영향을 받지 않습니다.

이것은 [이용허락규약\(Legal Code\)](#)을 이해하기 쉽게 요약한 것입니다.

[Disclaimer](#)

Thesis for the Degree of Master of Engineering

ZnS:Mn / PZT-based
Acoustic Electroluminescent Device

by

Wun Ho Lee

Department of LED Convergence Engineering

Specialized Graduate School Science and Technology Convergence

Pukyong National University

July 2017

ZnS:Mn / PZT-based
Acoustic Electroluminescent Device
(ZnS:Mn / PZT 기반 음향 출력 전계발광소자)

Advisor : Prof. Jong Su Kim

by
Wun Ho Lee

A thesis submitted in partial fulfillment of the requirements
for the degree of
Master of Engineering

Department of LED Convergence Engineering
Specialized Graduate School Science and Technology Convergence
Pukyong National University

August 2017

ZnS:Mn / PZT-based
Acoustic Electroluminescent Device

A dissertation

by

Wun Ho Lee

Approved by:

(Chairman) Yong Seok Jeong

(Member) Jong Su Kim

(Member) Yong Hyun Kim

August 2017

Contents

Abstract	i
I Introduction	1
II Background	4
1. Electroluminescence.....	4
1.1. Various electroluminescences (EL).....	4
1.2. Alternating Current Powder Electroluminescence Device (ACPELD).....	7
2. Phosphor of electroluminescence.....	9
2.1. Principles of electroluminescence.....	11
3. The piezoelectricity and dielectric property of device	14
3.1. Piezoelectric materials : PZT.....	14
III Experiment	16

1. Phosphor synthesis : ZnS:Mn ²⁺ phosphor.....	16
2. Acoustic electroluminescent device.....	18
2.1. Rear electrode substrate : Brass.....	18
2.2. Emissive layer : ZnS:Mn ²⁺ phosphor and organic binder	18
2.3. Dielectric layer : Lead zirconate titanate (PbTi _{0.48} Zr _{0.52} O ₃ , PZT).....	19
2.4. Transparent top electrode : Silver nanowires (Ag NWs)	20
2.5. Configuration of acoustic electroluminescent device	20

IV Results and Discussions..... 22

1. Structural characterization.....	22
1.1. Morphology of ZnS:Mn ²⁺ phosphor.....	22
1.2. XRD pattern of ZnS:Mn ²⁺ phosphor.....	24
2. Optical properties.....	26
2.1. Photoluminescence (PL)/PL excitation (PLE)/EL spectra	26
2.2. Decay curves.....	28

2.3. Transmittance of transparent electrode : Ag NWs	30
3. Opto-electric properties	31
3.1. Voltage-dependent EL spectra	31
3.2. Frequency-dependent EL spectra	34
3.3. Temperature-dependent EL spectra	38
3.4. Charge-voltage curves	40
4. Sound properties	42
4.1. Piezoelectricity	42
4.2. Configuration of acoustic EL device	42
4.3. Resonance frequency of acoustic EL device	44
4.4. Frequency and voltage-dependent sound pressure levels	47
4.5. Sound signals of acoustic EL device	51
V Conclusion	54
References	56
국문 요약	59

List of figures

Fig. 1. Categorization of electroluminescence.....	8
Fig. 2. General structures of alternative current powder electroluminescent devices.....	10
Fig. 3. Various electroluminescence spectra of phosphor using ZnS host.....	12
Fig. 4. Comet phase of ZnS electroluminescence in Fischer model.....	15
Fig. 5. The emission mechanism of ZnS:Mn, Cu including simultaneous injection of electrons and holes.....	15
Fig. 6. Piezoelectricity of lead zirconate titanate (PZT)....	17
Fig. 7. Synthesis process of ZnS:Mn ²⁺ phosphor.....	19
Fig. 8. Configuration of acoustic EL device.....	23
Fig. 9. SEM image of ZnS:Mn ²⁺ phosphor.....	25
Fig. 10. XRD pattern of ZnS:Mn ²⁺ phosphor; the	

bi-phase of cubic and hexagonal structures	27
Fig. 11. Normalized PL/PLE/EL spectra of ACPELD	29
Fig. 12. Fluorescence decay curve of ZnS:Mn ²⁺ emission	31
Fig. 13. Optical transmittance of transparent top electrode ; Ag NWs	32
Fig. 14. EL spectra of EL device for various applied voltages at 400 Hz	34
Fig. 15. Luminance-voltage (L-V) characteristics of EL device	36
Fig. 16. EL spectra of EL device for various frequencies at 150 V	37
Fig. 17. Luminance-frequency (L-F) characteristics of EL device	39
Fig. 18. Luminance-temperature (L-T) characteristics of EL device	41
Fig. 19. Charge-voltage (Q-V) characteristics of EL device	43
Fig. 20. Configuration of acoustic EL device	45
Fig. 21. Sound spectrum of acoustic EL device for various frequencies including resonance frequency	48
Fig. 22. Frequency dependent SPL of acoustic EL device	50

Fig. 23. Voltage dependent SPL of acoustic EL device.....52

Fig. 24. Sound signal outputs of acoustic EL device in frequency domain; (a) $f_0=110$, (b) $f_0=220$, (c) $f_0=440$ and (d) $f_0=880$ Hz. The insets shows time-domain sound signals..... 54



ZnS:Mn / PZT-based Acoustic Electroluminescent Device

Wun Ho Lee

Department of LED Convergence Engineering
Specialized Graduate School Science and Technology Convergence
Pukyong National University

Abstract

A novel electroluminescent (EL) device which emits sound as well as light, acoustic EL, has been achieved by using piezoelectric material as dielectric layer. This acoustic EL device consists of silver nanowires as top electrode, and ZnS:Mn²⁺ phosphor screen-printed on high piezoelectric material lead zirconate titanate (PZT) ceramic sheet. The ZnS:Mn²⁺ phosphor was synthesized by solid state reaction method. The PZT ceramic sheet has high piezoelectric coefficient (d_{33}) as well as high dielectric constant (k). The high d_{33} value (~ 400 pC/N) resulted in high sound pressure level up to 83 dB at 100 V and 3,400 Hz. The high k value (~ 1650) caused to the high EL luminance up to about 2 cd/m² at 350 V and 400 Hz. The EL luminances was

exponentially dependent on the applied voltage while the sound pressure levels was linearly dependent on the applied voltage, with the same threshold voltage of 50 V. The EL luminances was linearly increased and then saturated at the inverse of the decay time (~ 600 Hz) with increasing the applied frequency while the sound pressure levels showed the flat response below 600 Hz and then parabolic increase above 600 Hz. The temperature-dependent EL luminances were maximized at the temperature of 160 °C, which is consistent with Curie temperature of the PZT sheet.

keyword : Electroluminescent device, Piezoelectric device, ZnS:Mn²⁺ phosphor, Lead zirconate titanate (PZT)

I Introduction

The powder electroluminescence (EL) device consists of a transparent top electrode on a substrate, a phosphor layer and a dielectric layer dispersed in an organic binder and a bottom electrode [1]. The EL phenomenon is attributed to phosphor excitation by hot electrons injected from the dielectric layer to the phosphor layer when a high electric field of order of magnitude of 10^6 V/cm is applied to the phosphor layer [2]. The most of ZnS-based phosphors are commercially available for powder EL: blue ZnS:Cu, Cl green ZnS:Cu, Al and orange ZnS:Cu, Mn [3]. Powder EL devices have non-glare uniform light emission, thin profile of about 200 μm and low power consumption of about 30 W/m^2 for a luminance of about 100 cd/m^2 [3]. Powder EL devices are used for liquid crystal display (LCD) backlight, and architectural and decorative lighting. One interesting EL

application is the display panel for very harsh environments such as space modules and fighting vehicles due to high thermal stability over the temperature range of $-50/+100$ °C [3]. Other interesting EL modification is the sound-generating EL device based on piezoelectric dielectric layer [4]. However, the BaTiO_3 dielectric used for commercially available EL devices has lower piezoelectric properties and a lower Curie temperature [3, 4]. Thus, the lead zirconate titanate (PZT) material in this experiment is selected as a dielectric layer due to its high dielectric and piezoelectric properties [5, 6]. By using the piezoelectric PZT layer as a dielectric layer in the EL device, the acoustic output is obtained when a high voltage sinusoidal wave is applied. The PZT layer in the EL device has two functions. First, it works as a dielectric layer to prevent the electric breakdown between electrodes and maximize the efficiency of EL emission. Secondly, it functions as piezoelectric vibrator under AC voltage to generate the sounds. The bi-functional EL device on PZT dielectric layer, which generates lights and sounds, leads to the expectation to new type applications

by combination of various technologies [3-5].

In this study, a novel electroluminescent (EL) device which emits sound as well as light, acoustic EL, has been achieved by using piezoelectric material as dielectric layer. This acoustic EL device consists of silver nanowires as top electrode, and ZnS:Mn²⁺ phosphor screen-printed on high piezoelectric material lead zirconate titanate (PZT) ceramic sheet. The ZnS:Mn²⁺ phosphor was synthesized by solid state reaction method. The fabricated EL device exhibits the orange-yellow electroluminescence with a high EL luminance of 2 cd/m² at 350 V and 400 Hz as well as the high sound pressure level up to 83 dB at 100 V and 3,400 Hz. The temperature-dependent EL luminances were maximized at the temperature of 160 °C, which is consistent with Curie temperature of the PZT sheet. Finally our EL device generated the lights from the phosphor as well as the sounds from PZT sheet with high thermal stability, so that it can be used as large-scale sheet-type EL speaker.

II Background

1. Electroluminescence

1.1. Various electroluminescences (EL)

Electroluminescence (EL) is the generation of light by the application of an electric field to crystalline materials, or resulting from a current flow through semiconductors. The EL of inorganic materials is classified into the two groups: injection EL and high electric field EL. The high-field EL is divided into two types: powder phosphor EL and thin film EL. The classification of EL is summarized as seen in figure 1 [7]. Historically, the EL phenomenon was first observed by Destriau in 1936, who observed luminescence produced from ZnS powder phosphors suspended in castor oil when a

strong electric field was applied. This type of EL is classified as powder phosphor EL. In the early 1960s, polycrystalline ZnS thin films were used as EL materials. This type of EL is typical of thin-film EL. On the other hand, in 1952 infrared EL from forward biased p-n junctions in Ge and Si diodes was reported. This type of EL is classified as injection EL. Visible EL is observed in diodes made of wide band gap semiconductors, such as GaP. These diodes are called light-emitting diodes (LEDs) and have been widely used since the late 1960s. In 1987, C.W. Tang reported that the organic LED (OLED) was based on Alq₃ organic emissive layer. These OLED have been widely used for display since the 2000s. The mechanisms of light generation in injection EL and high-field EL are quite different from each other. In addition, the applications of these EL phenomena to electronic devices are different. Usually, the term EL is used, in a narrow sense, to mean high-field EL. In this thesis, the works will focus on the basic processes of the high-field EL, in particular on the excitation mechanisms in powder EL.

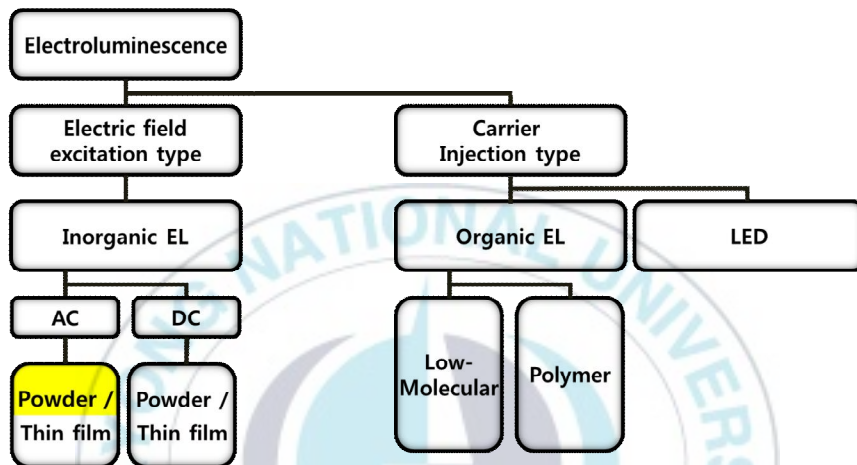


Figure 1. The categorization of electroluminescence

1.2. Alternating Current Powder Electroluminescence (ACPELD)

The first high-field EL phenomenon was discovered by Destriau in 1936 [1]. It was the AC EL phenomenon based on the ZnS phosphor powder immersed in an oil and inserted between two electrodes to emit light by application of an AC voltage. The AC powder EL device has some advantages: high thermal and vibrational stabilities due to a perfect device of solid-state condition. The EL device is driven at low consumption, and it can be made thin and light. Therefore various applications in various fields are expected. Figure 2 shows the general structure of AC powder EL device (ACPELD) including both emissive and dielectric layers when AC voltage is applied [8].

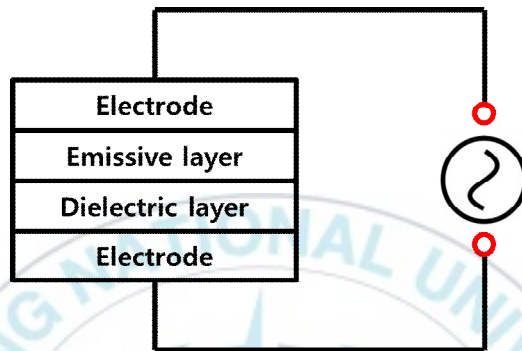


Figure 2. General structure of alternative current powder electroluminescent device

2. Phosphors of electroluminescence

The conditions of the host material used for the emitting layer of the EL devices should be (1) transparent in the visible region by adding an appropriate light-emitting center, and (2) stable in a high electric field necessary for the EL emission. For these reasons, the EL host materials have kinds of semiconductors with a relatively large band gap as well as doped with an appropriate luminescence center (activator, color center). The host materials that has already been put to practical use is ZnS. The luminescence of doped ZnS:Mn²⁺ phosphor is an orange-yellow color having a broad peak due to the forbidden transition of Mn²⁺ ions. Figure 3 shows the emission spectra of the phosphor with ZnS host. By doping some different luminescent center, various luminescent colors are obtained in the visible region [9].

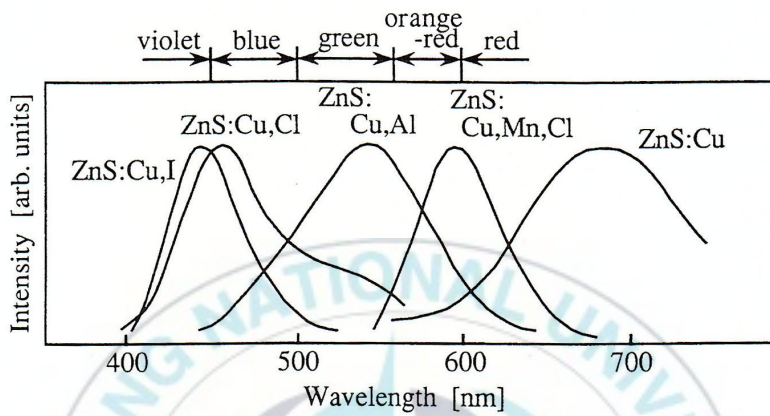


Figure 3. Various electroluminescence spectra of phosphor using ZnS host

2.1. Principles of electroluminescence

The light emitting layer (phosphor layer) is made by dispersing the phosphor powder in an organic binder : ZnS as the host material of the phosphor powder and Al^{3+} and Cu^{2+} ions as the activator to gain the orange-yellow color. The particle size of the ZnS phosphor is around 5 ~ 30 μm . The organic binder is cyano ethylcellulose, that is, an organic material having a relatively high dielectric constant. A dielectric layer is formed between the emitting layer and the rear electrode to prevent dielectric breakdown, and the metal sheet is used for the rear electrode. The Fischer model is generally cited for the principle of luminescence of the powder-type AC EL device [10, 11]. Figure 4 shows the EL emission principle of the ZnS phosphor proposed by Fisher. When an electric field is applied, the luminescent region gradually becomes larger, and the luminescent region becomes like a comet that faces each other.

Figure 5 shows the fundamental EL mechanism of ZnS:Cu, Al phosphor. Adjacent Cu^{2+} precipitates along the

line defects in the ZnS grains so as to form Cu_xS with a large p-type conductivity and its heterojunction with n-type ZnS [10]. Electrons and holes are injected into the ZnS from the surface level due to the tunnel effect under the high electric field, and they recombine so as to cause electroluminescence [11, 12].

The relation between the luminance L and the voltage V is given by here [13] ;

$$L = L_0 \exp(-(V_0/V)^{-1/2}) \dots\dots\dots (1)$$

L_0 and V_0 are constants, which depend on the particle size of the phosphor, the concentration of the activator, the thickness of the light emitting layer, and the dielectric constant of the organic binder.

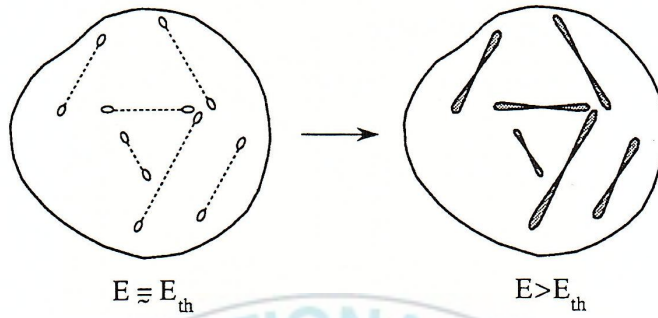


Figure 4. Comets phase of ZnS electroluminescence proposed by Fischer

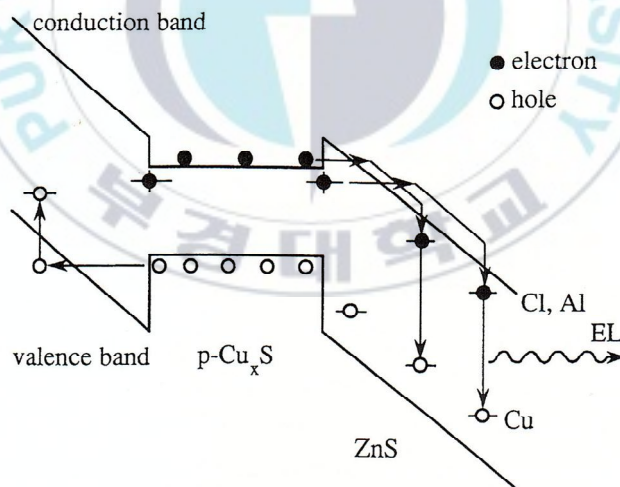


Figure 5. The fundamental EL mechanism of ZnS:Cu, Al including simultaneous injection of electrons and holes

3. The piezoelectricity and dielectric property of device

3.1. Piezoelectric materials : PZT

The piezoelectricity are related to pressure and electricity within a particular materials. The piezoelectric materials are materials that generate a voltage when a mechanical stress is applied or exhibit a dimensional change when an electric field is applied [14]. Thus, by using the piezoelectric PZT layer as a dielectric layer in the EL device, the acoustic output is obtained when a high voltage sinusoidal wave is applied. The well known dielectric material for the EL device is BaTiO₃ with the highest dielectric constant of about 10,000, which is comparatively weak in piezoelectric property. The PZT material in this experiment is selected as a dielectric layer due to its high dielectric and piezoelectric properties. The PZT layer in the EL device has two functions. First, it works as a dielectric

layer to prevent the electric breakdown between electrodes and maximize the efficiency of EL emission. Secondly, it functions as piezoelectric vibrator under AC voltage to generate the sounds. Figure 6 shows the piezoelectric properties of the PZT material showing the mechanical change (lattice expansion) when an electric field (E) is applied under Curie temperature (T_c) [15].

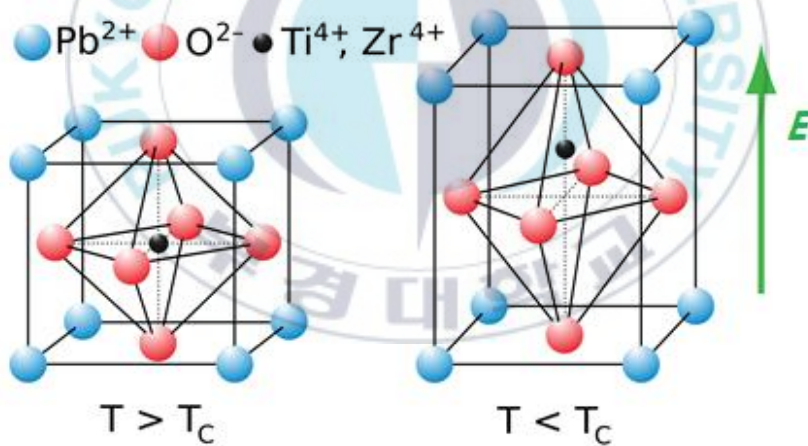


Figure 6. Piezoelectricity of lead zirconate titanate (PZT)

III Experiment

1. Phosphor synthesis : ZnS:Mn²⁺ phosphor

ZnS:Mn²⁺ phosphor were synthesized by solid-state reaction method. Zinc sulfide (ZnS) as host and manganese (Mn²⁺), copper (Cu²⁺) as dopants were sintered in the form of powder. 1 mol % of MnS and 0.1 mol % of CuS were mixed with ZnS powder. The mixture was filled at low vacuum condition in the high cleaned quartz tube. It was sintered at 900 °C for 3 hours and then cooled rapidly to obtain the bi-phase (cubic and wurtzite structure). The obtained synthetic product was powders of white body color. To observe particle size and shape of ZnS:Mn phosphor, scanning electron microscope (SEM) (Tescan, VEGA II LSU) was employed. To identify the crystal structure of

ZnS:Mn²⁺ phosphor, X-ray diffraction (XRD) pattern was measured from $2\theta^\circ = 20$ to 80° by using a X-ray diffractometer (Rigaku, Ultima IV). The photoluminescence excitation (PLE) spectrum, and fluorescence decay curves of ZnS:Mn²⁺ phosphor was measured by using a fluorescence spectrophotometer (Hitachi, F-4500).

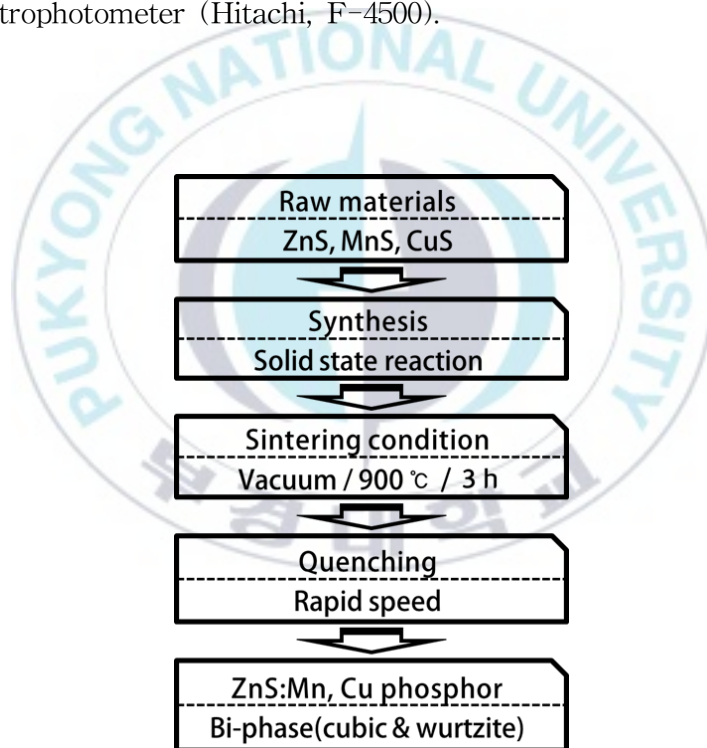


Figure 7. Process of ZnS:Mn²⁺ phosphor synthesis

2. Acoustic electroluminescent device

2.1. Rear electrode substrate : Brass

A type of fine metal was selected as the substrate due to low electric resistivity and high stiffness for amplification of piezoelectric vibration.

2.2. Emissive layer : mixture of ZnS:Mn²⁺ phosphor and organic binder

The ZnS:Mn²⁺ phosphor powder was dispersed in cyanoethyl cellulose as organic binder. The binder was accomplished for sufficient vehicle to take in phosphor. It had highest dielectric property of various resin-type binders. The mixture was two times printed on the dielectric PZT/brass substrate by a screen printing method. In this study, the optimized thickness of the phosphor layer (emissive layer)

was 40 μm for lower threshold voltage and high luminous efficiency.

2.3. Dielectric layer : Lead zirconate titanate

($\text{PbTi}_{0.48}\text{Zr}_{0.52}\text{O}_3$, PZT)

The Lead zirconate titanate (PZT) has two functions. The one is dielectric property and the other is piezoelectric property. In this study, It needs high dielectric constant to increase EL emission intensity. Also It requires high piezoelectric constant (d_{33}) to show high sound pressure level. Lead zirconate titanate (PZT) satisfied these requirements. In this experiment, 200 μm -thick PZT sheet (Murata's buzzer) was used: piezoelectric charge constant $d_{33}= 400 \text{ pC/N}$, dielectric constant (k) = 1650

2.4. Transparent top electrode : Silver nanowires (Ag NWs)

The silver nanowires were dissolved in deionized water. The colloidal solution was mixed with hydroxypropyl methylcellulose (HPMC) with mixture ratio of 45 % and 10 % in were dispersed in deionized water. The definitive solution was spin-coated on the ZnS:Mn²⁺ phosphor layer. The coated silver nanowires were dried at 100 °C for 50 minutes. The transparency of coated silver nanowires transparent electrode was measured from 300 nm to 900 nm using a UV-Vis spectrophotometer (Lambda 40, Perkin Elmer). The resistivity of silver nanowires electrode was measured by Van Der Pauw method.

2.5. Configuration of acoustic electroluminescent device

The electroluminescent properties of EL device was measured using spectrophotometer (Konica minolta, CS-2000).

Charge density versus applied voltage (Q-V) characteristic of EL device was measured using Sawyer-Tower circuit. The piezoelectric properties of EL device was measured by (IACAS, piezo meter). Sound pressure levels (SPLs) in dB unit were measured with a distance of 1 cm between the EL device and the microphone. Time and frequency-domain acoustic spectra was analyzed by a program of Gold Wave.

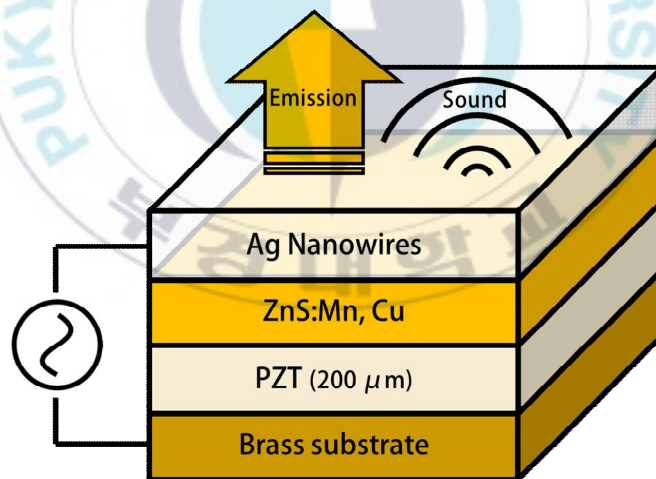


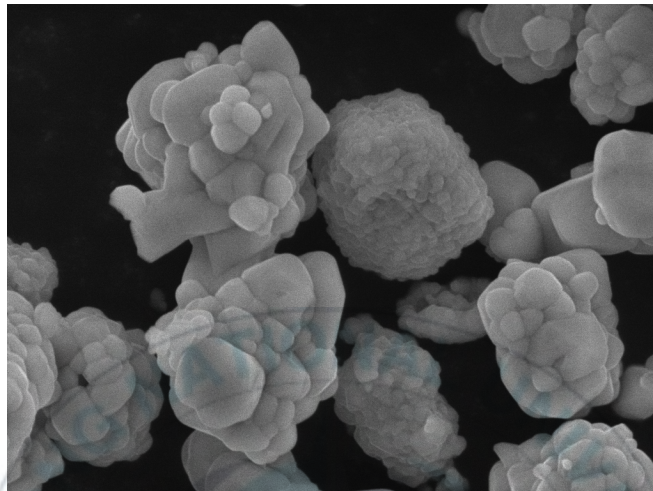
Figure 8. Configuration of acoustic EL device

IV Results and discussion

1. Structural characterization

1.1. Morphology of ZnS:Mn²⁺ phosphor

Figure 9 shows SEM image of ZnS:Mn²⁺ particles synthesized by a solid-state reaction. Smaller particles with an average size of around 1 ~ 2 μm aggregate to be spherically shaped. The bigger particles have an average size of around 5 μm.



SEM HV: 15.00 kV SEM MAG: 15.00 kx VEGAII TESCAN
Det: SE 5 μm PKNU

Figure 9. SEM image of ZnS:Mn²⁺ phosphor

1.2. XRD pattern of ZnS:Mn²⁺ phosphor

Figure 10 shows the XRD pattern of ZnS:Mn²⁺ phosphor. The ZnS:Mn²⁺ phosphor has two structures: cubic and hexagonal (wurtzite) structures. It is confirmed that our phosphor is bi-phased, or two phases coexist. Cubic phase-based three main diffraction peaks from (111), (200) and (311) planes (JCPDS card No. 77-2100) are observed. Wurtzite structure (JCPDS card No. 75-1547) is also detected. According to the ratio of the maximum XRD intensities of cubic and hexagonal phases, the ratio of total amounts of two phases are 90:10.

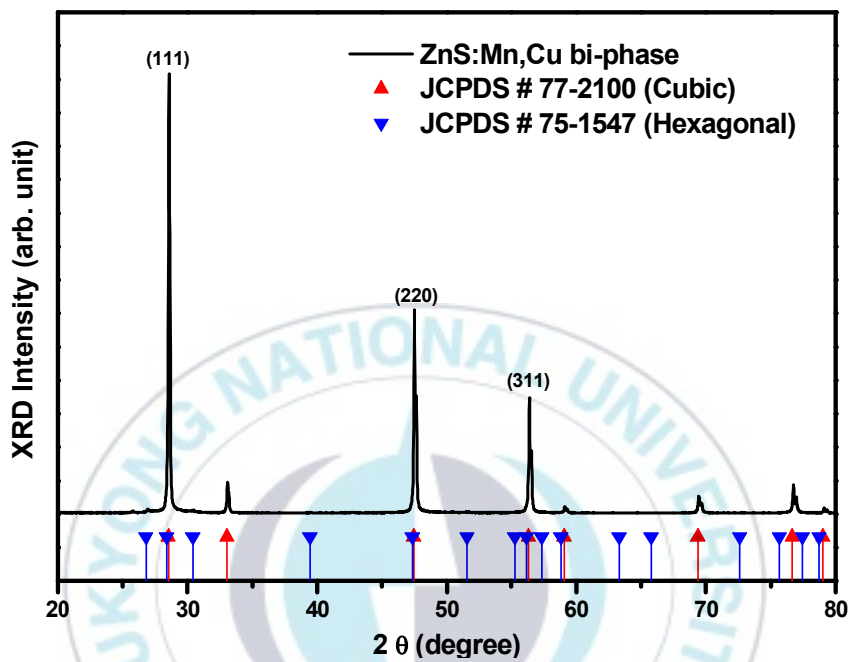


Figure 10. XRD patterns of ZnS:Mn²⁺ phosphor ;
the bi-phase of cubic and hexagonal structures

2. Optical properties

2.1. Photoluminescence (PL)/PL excitation (PLE) / EL spectra

Figure 11 shows photoluminescence (PL) and photoluminescence excitation (PLE) spectra of ZnS:Mn²⁺ phosphor. The PLE spectrum has 342 nm peak, which results from band-band transition. The PL spectrum shows 581 nm peak, which results from the ${}^4T_1 - {}^6A_1$ transition of Mn²⁺ ion in ZnS:Mn²⁺ [16]. The EL spectrum at 200 V and 400 Hz shows 583 nm peak, which is slightly shifted compared with 581 nm PL peak. These redshift of EL spectrum is attributed to the Joule heating effect by a current of hot electrons in EL device.

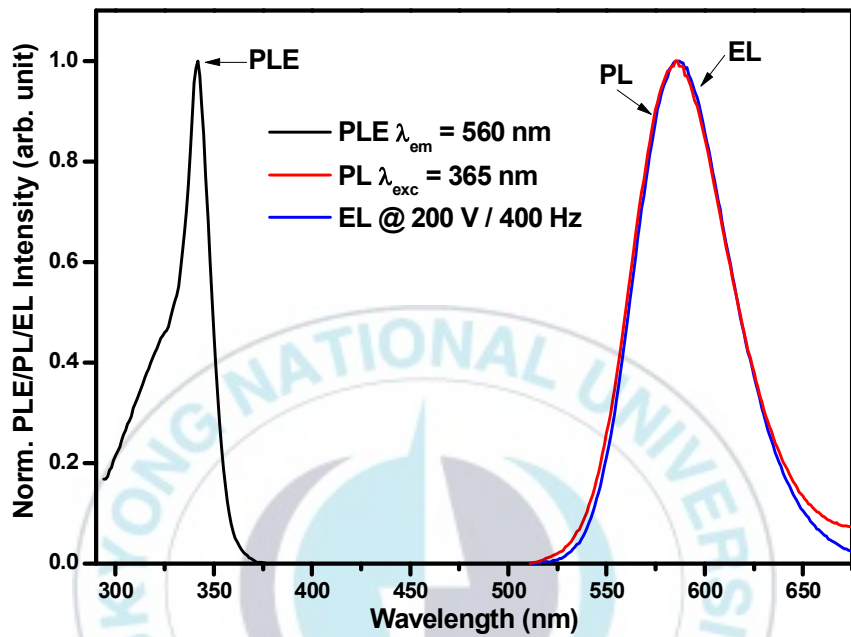


Figure 11. Normalized PL/PLE/EL intensity of ACPELD

2.2. Decay curves

Figure 12 shows the decay curve of 581 nm main PL peak of ZnS:Mn²⁺ phosphor. It is known that the phosphor with a low concentration of a single kind of Mn²⁺ dopant has an exponential decay curve with a decay time of a millisecond order due to ⁴T-⁶A forbidden transition of 3d⁵ orbital of Mn²⁺ ion [16]: $I \propto e^{-t/\tau_0}$, τ_0 is defined as the decay time. In the case of our phosphor doped with 1 mole% of Mn²⁺, its decay time is around 1.7 ms as a fitting result of the exponential decay function. This millisecond decay time can cause to saturating the EL intensity at the critical applied frequency which is estimated to be proportionally inverse of decay time. The EL device shows the saturation behavior of the EL intensity at the critical frequency of about 600 Hz, which is confirmed in EL intensity dependence on frequency as follows.

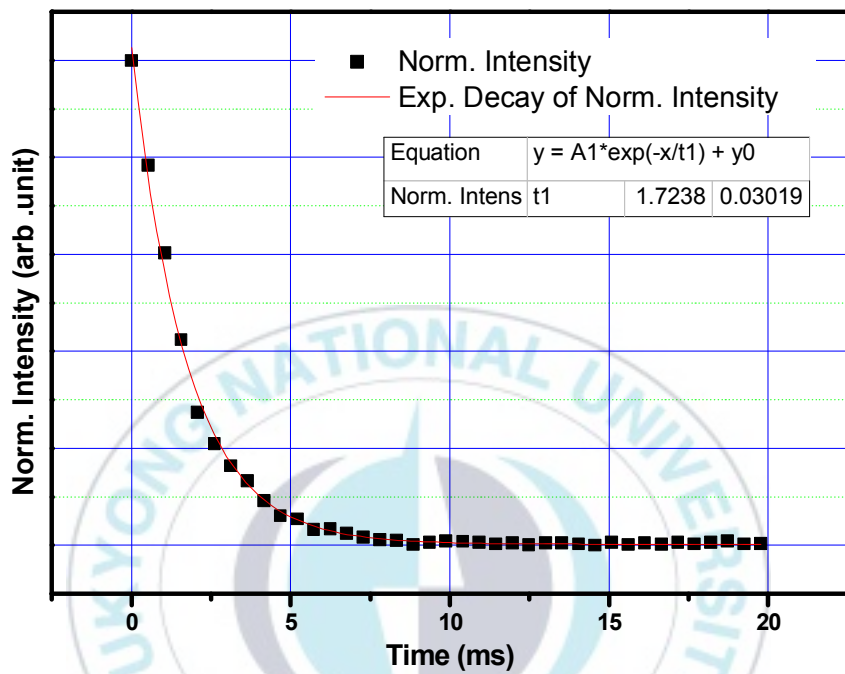


figure 12. Fluorescence decay of ZnS:Mn²⁺ emission

2.3. Transmittance of transparent electrode : Ag NWs

Figure 13 shows the transmittance spectrum of silver nanowires (Ag NWs) coated on slide glass substrate as transparent top electrode. It shows an excellent transparency with a transmittance of 83 % at the 583 nm wavelength which correspond to the EL peak. Also it has a low sheet resistance of 6 Ω /sq which is good to be used for the transparent electrode.

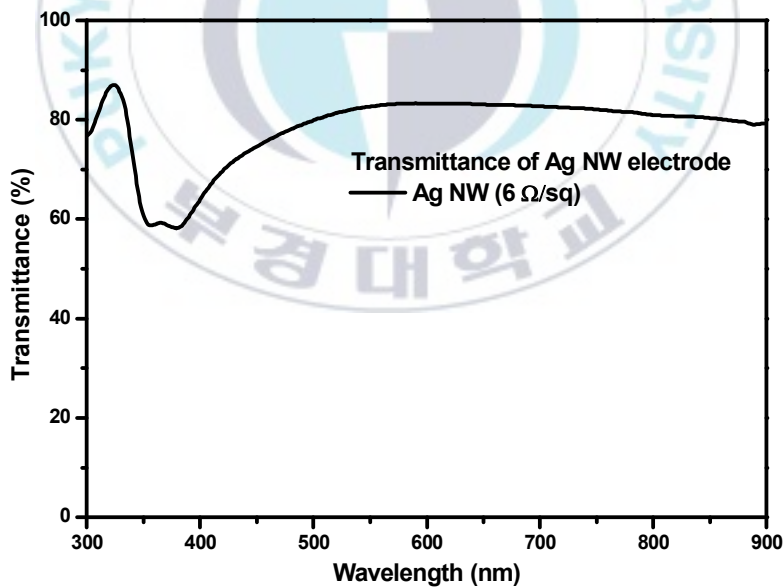


figure 13. Optical transmittance of transparent electrode ; Ag NWs

3. Opto-electric properties

3.1. Voltages-dependent EL spectra

Figure 14 shows EL spectra of EL device varying from 75 to 325 V for a fixed frequency of 400 Hz. The peak wavelength is 583 nm and the full width at half maximum (FWHM) is 61 nm. The CIE color coordinate are $x = 0.5436$ and $y = 0.4497$. The EL spectra are unchanged with increasing of the applied voltages. On the contrary, the blue-green emission color of the conventional ZnS:Cu, Al-based EL device is strongly dependent on the excitation frequency: the blue shift at higher voltage. The EL emission peak is assigned to the transition from the lowest state (4T_1) to the ground state (6A_1) in $3d^5$ manifold of Mn^{2+} ion [17]. In addition, the EL spectrum is slightly broader and red shifted than the photoluminescence (PL) spectrum of ZnS:Mn²⁺ phosphor, as shown in figure 11. It is due to the heating effect of EL device by the hot electrons which make the impact excitation of Mn²⁺ ions.

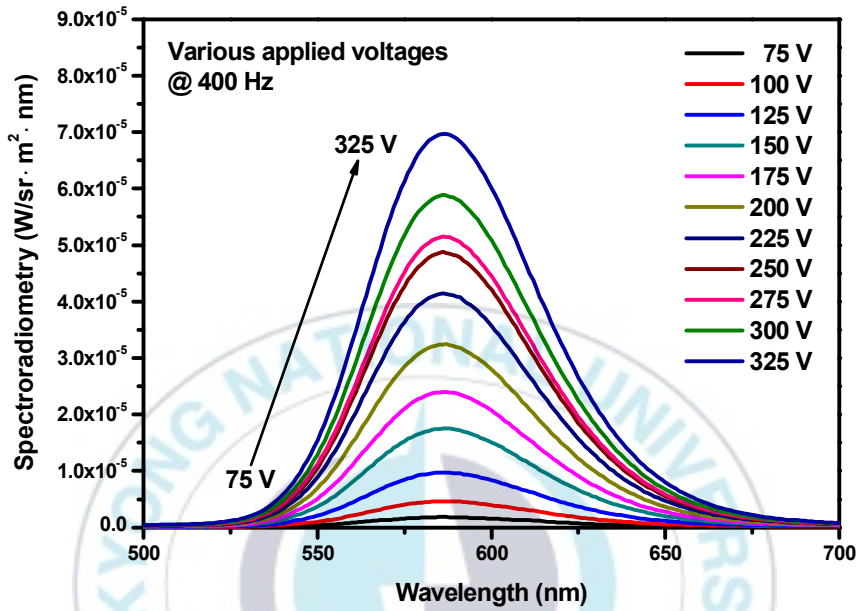


figure. 14. EL spectra of EL device for various applied voltages at 400 Hz

The EL device was driven by a sinusoidal power at various applied voltages. The threshold voltage (V_{th}) of the device could be determined about 50 V. The electric field in the phosphor layer is calculated as 2.1×10^5 V/cm (~ 50 V / 240 μ m). In the conventional powder EL devices, the luminance is given [18].

$$L = L_0 \exp(-(V_0/V)^{-1/2}) \dots\dots\dots (1)$$

L_0 and V_0 are constants, which depend on the particle size of the phosphor, the concentration of the activator, the thickness of the light emitting layer, and the dielectric constant of the organic binder. The equation reveals that the logarithm of L is directly proportional to $V^{-1/2}$. Luminance (L) versus applied voltage ($V^{-1/2}$) varying from 75 to 350 V at a fixed frequency of 400 Hz is plotted in figure 15. The experimental results are roughly in accordance with the above equation. It suggests that the excitation mechanism of the powder EL of the ZnS:Mn²⁺ phosphor is similar with that of the conventional ZnS:Cu, Al phosphors. A luminance of 2.05 cd/m² was obtained at 350 V and 400 Hz.

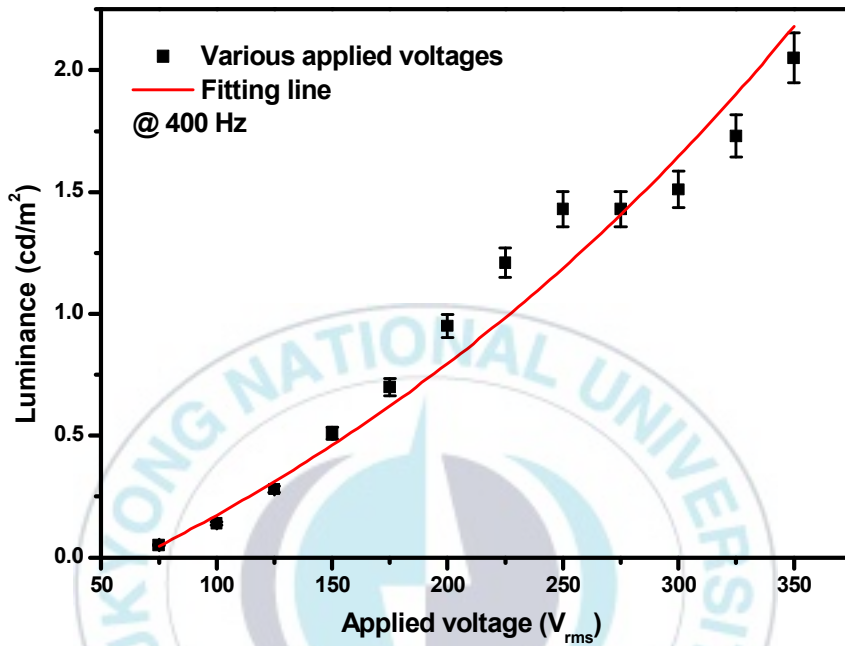


Figure 15. Luminance-voltage ($L-V$) characteristics of EL device

3.2. Frequencies-dependent EL spectra

Figure 16 displays EL spectra at the various frequencies from 50 Hz to 1000 Hz for a fixed voltage of 150

V. The EL spectra are independent on the frequency. On the contrary, the excitation frequency of the commercial green EL device using ZnS:Cu, Al phosphor causes to the blueshift of its emission color.

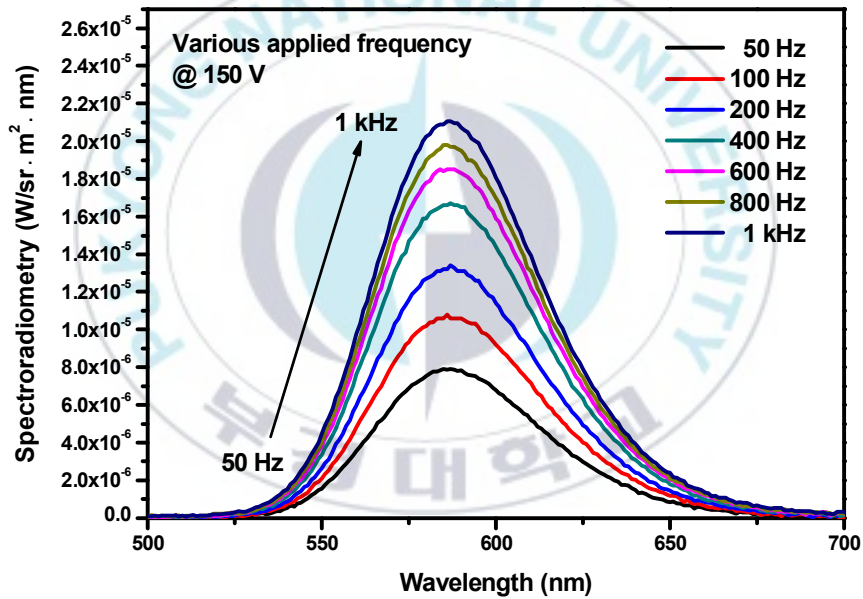


Figure 16. EL spectra of EL device for various frequencies at 150 V

At lower frequency, the luminances are linearly increased. This trend can be explained by the increasing chances of excitation of the host lattice or Mn^{2+} ions with increasing frequency. At higher frequency, the luminances are saturated. This is the reason why ZnS:Mn^{2+} phosphor has a long decay time due to the forbidden transition of Mn^{2+} ions so that the EL excitation happens before the full decay of its emission, that is, within the decay time of millisecond order. The saturation frequency (f_s) can be approximately defined as the inverse of the decay time (τ) : $1/\tau = 1/1.7 \text{ ms} = f_s \approx 600 \text{ Hz}$. This value is consistent with our result. That is shown figure 17.

Finally we can conclude that the ZnS:Mn^{2+} -based EL device is not spectrally influenced by both frequency and applied voltage, and it possesses higher stability in operation condition.

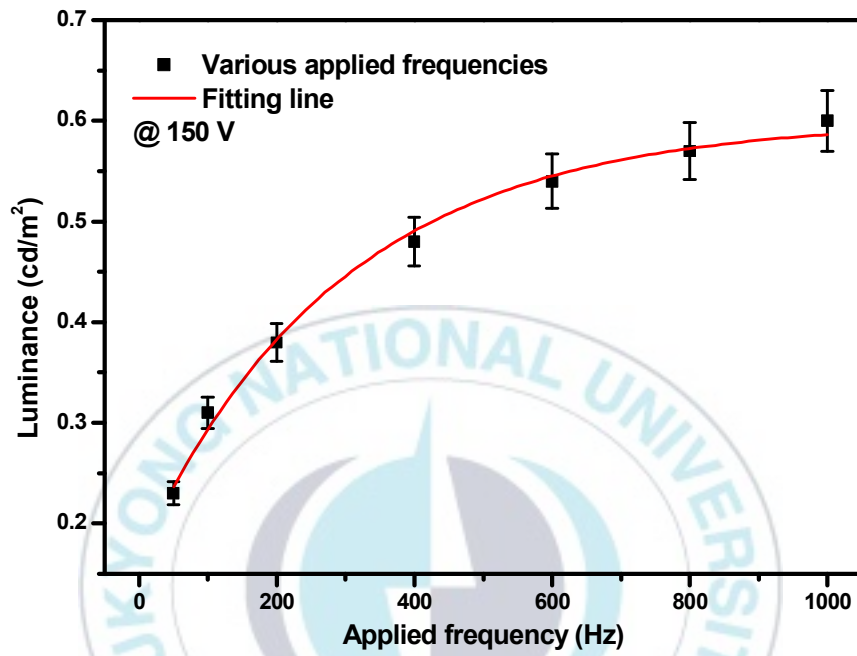


Figure 17. Luminance–frequency (L – F) characteristics of EL device

3.3. Temperature dependent EL spectra

Figure 18 shows the temperature dependent EL spectra of EL device at the sinusoidal voltage of 200 V and frequency of 400 Hz. As an increase of temperature, PL intensities are linearly decreased. On the other hand, the EL intensities slightly decreased at lower temperature, and then drastically increased and reached the maximum intensity around 180 °C, and then significantly quenched. The phosphor does suffer from the thermal quenching effect and the drastic enhancement of the EL intensities results not from a thermal variation in the phosphor but from other effect, that is, the temperature dependence of dielectric constant of PZT layer. In a conventional dielectric material such as PZT, its dielectric constant is reported to be maximized at the Curie temperature and then drastically decreased. Ignoring the thermal quenching effect of the phosphor, the temperature dependence of our EL device using PZT dielectric layer follows the temperature dependence of its dielectric constant (k)

$$k = C*d/\epsilon_0A \dots\dots\dots (2)$$

while C is capacitance, d is thickness, ϵ_0 vacuum permittivity and A is dielectric surface area. Based on the equation (2) the PZT dielectric constant is around 1,650.

Finally we can conclude that the ZnS:Mn²⁺ / PZT-based EL device is not degraded in the EL intensity under a hot ambient temperature, and it shows higher stability in an extreme operation condition.

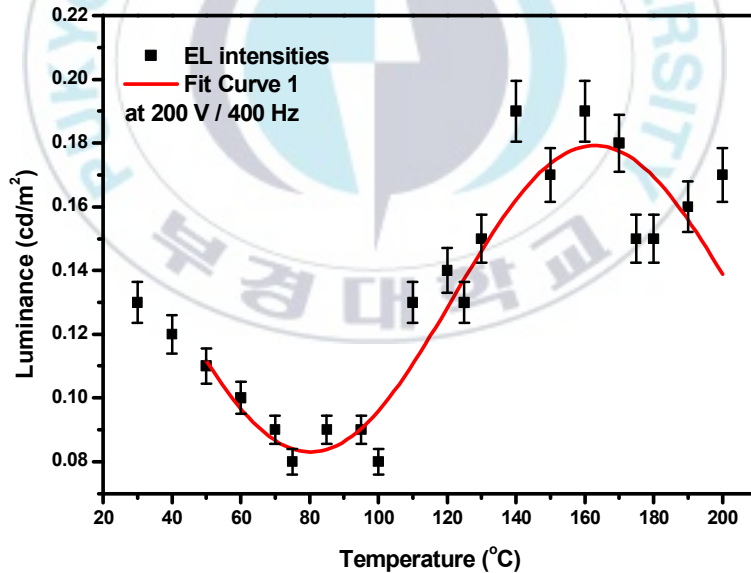


Figure 18. Luminance-temperature ($L-T$) characteristics of EL device

3.4. Charge–voltage curves

Figure 19 depicts charge density (Q) versus applied voltage (V) at the sinusoidal voltages from $50 V_p$ to $200 V_p$ and frequency of 400 Hz. The $Q - V$ diagram is based on a conventional Sawyer–Tower circuit using sense capacitor with a capacitance of $0.98 \mu\text{F}$ at 400 Hz. As an increase of voltage, the remaining charge densities at the transient voltage of zero are increased from 14 at 50 V to 125 nC/cm^2 at 200 V. The charge density reaches maximum of 201 nC/cm^2 at $152 \sim 168 V_p$ in the falling phase of applied voltage. The integrated area (A) of the $Q - V$ diagram means the power consumption to the EL device per one cycle. The full power consumption and the luminance are measured and values of 300 W/m^2 and 0.75 cd/m^2 are obtained at the voltage $200 V_p$ and 400 Hz. Assuming a diffusive EL emission surface of EL device, the luminous efficiency (η) is given by ;

$$\eta [\text{lm/W}] = \pi L [\text{cd/m}^2] / f [\text{Hz}] \times A [\text{W/m}^2] \quad (3)$$

where L is the luminance in the unit of cd/m^2 , and f is the

frequency in the unit of Hz, and A is the encompassed area of Q - V diagram in the unit of W/m^2 . So, the luminous efficiency (η) is 0.007 lm/W .

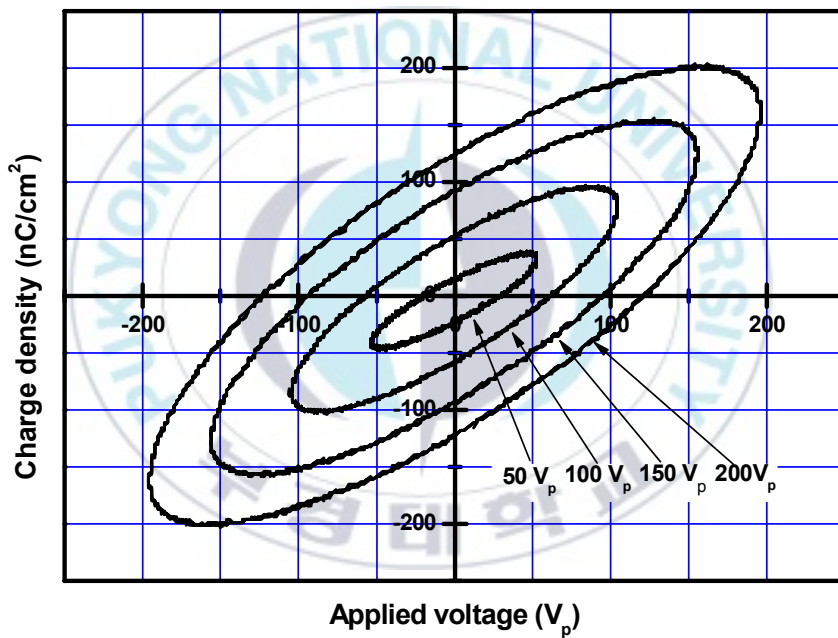


Figure 19. Charge-voltage (Q - V) characteristics of EL device

4. Sound properties

4.1. Piezoelectricity

The Murata's 200 μm -thick PZT ceramic was measured the piezoelectric charge constant $d_{33} \sim 400$ pC/N and the dielectric constant $k \sim 1650$. These values are close to the PZTs used in commercial piezoelectric speakers [19].

4.2. Configuration of acoustic EL device

The schematic configuration of our acoustic EL device is shown in figure 20. The circular brass metal as a vibration plate is 27 mm in diameter and 0.3 mm in thickness. The circular PZT ceramic sheet is 19 mm in diameter and 0.2 mm in thickness. The square phosphor layer on the PZT sheet is 13 mm in length and 40 μm in thickness, and the Ag NW layer as the top electrode is

coated on the phosphor layer in the same shape. The total mass of the acoustic EL device is 1.98 g, which includes the glue between the PZT sheet and vibration plate, and Ag paste between the Ag NW layer and connection wire.

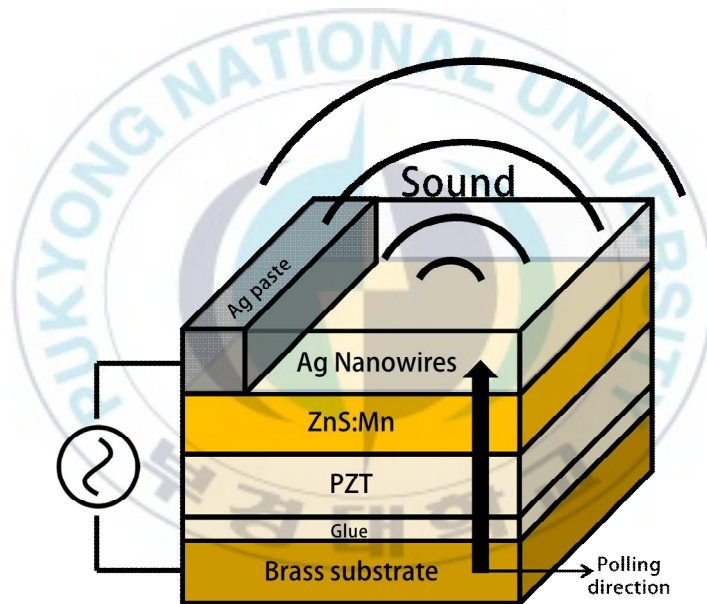


Figure 20. Schematic configuration of acoustic EL device

4.3. Resonance frequency of acoustic EL device

In piezoelectric speakers the resonance frequency depends on the method used to support the piezoelectric diaphragm: node support, edge support, and central support. The acoustic EL device were tested in the edge support of its circular vibration plate edge by the Audio Tester system. The distance between the microphone and the EL device was 1 cm, and the various applied voltages of less than the breakdown voltage of 250 V with sin signal within a band of 110 Hz – 4,400 Hz was used to drive the acoustic EL device.

The fundamental resonance frequencies (f_r) is determined by the material properties as follows :

$$f_r \propto (m/k)^{1/2} \dots\dots\dots (4)$$

where m is the mass and k is related to the elasticity coefficient which is influenced by the structure. The weight of the PZT sheet and vibration plate is ~ 1.97 g, which is the dominate part in weight. The values of the mass including the phosphor layer are 1.98 in the unit of $\text{kg}^{1/2}$.

The most severe drawback of piezoelectric speakers is known to be their poor sound radiation performance in the low frequency region. It is attributed to the diaphragm such as PZT sheet and metal plate being too stiff to vibrate with large amplitude. Thus, the f_r value of our EL speaker is too large to be practically used. The more works on reducing the value is required as follows.

According to Equation (4) two methods can be suggested in the aspect of material science. First method is the decrease of the total mass (phosphor layer + PZT sheet) by controlling their thicknesses, for example, the decrease of the current PZT thickness of 200 μm up to the order of 10 μm leads to the reduction of the f_r value. However our structure has similar weight compare to PZT sheet which is only has 0.01 g different. But the addition of phosphor and binder make the elasticity coefficient increased. So our acoustic resonance frequency is 3,400 Hz or lower than PZT sheet ($\sim 4,600$ Hz) which shown on figure 21.

Second method is to increase the d_{33} , especially, the d_{33} of the phosphor layer by optimizing densities and kinds

of organic binders and phosphors. Based on the measurement result of piezo d_{33} meter, d_{33} coefficient of PZT with phosphor is 40 pC/N, which is lower than only PZT sheet with 400 d_{33} coefficient value. It is caused by the phosphor layer including organic binder with a low d_{33} coefficient value which make d_{33} coefficient value of the acoustic EL device lower. With the decreasing of d_{33} coefficient value the maximum sound the acoustic EL device was by 20 % (20 dB) decreased compared to pure PZT sheet (100 dB).

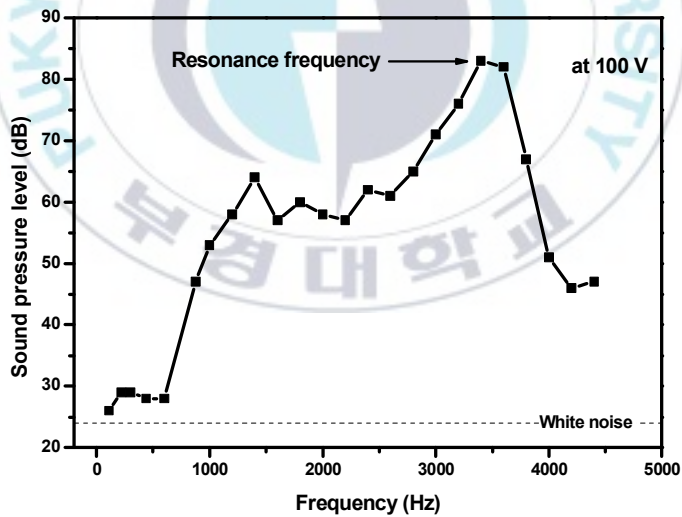


Figure 21. Sound spectrum of acoustic EL device for various frequencies including resonance frequency

4.4. Frequency and voltage-dependent sound pressure levels

Frequency response of an ideal piezoelectric speaker can be modeled as a single-resonance system. Below f_r , the SPL is proportional to the square of the frequency ($\sim f^2$) because the displacement of vibrator is inversely proportional to the signal frequency. Above f_r , the SPL is approximately independent of the frequency. Figure 22 shows below the frequency of about 600 Hz, the frequency response of our EL speaker is flat, which is independent on the frequency. This violation of the rule of the model is considered to be due to the existence of the non-piezoelectric phosphor layer on the PZT sheet. Above the frequency of about 600 Hz, the frequency response follows the as-mentioned single-resonance mode 1 : $SPL \sim f^2$.

The SPL of the speaker is expressed by the following equations [20] :

$$SPL = 10 \log 10 (I/I_{ref}) \dots\dots\dots (5)$$

where I is the intensity of the sound and I_{ref} is the intensity

of the reference, which is 20 μPa . Moreover, $I = (P_m/2^{1/2})^2/(\rho c)$, where P_m is the maximum amplitude of the sound wave which is generated by the piezoelectric ceramics, while ρ is the density of the medium and c is the velocity of the sound wave in the medium. Therefore, SPL was increased with the increase of the amplitude of the vibration of the piezoelectric ceramics.

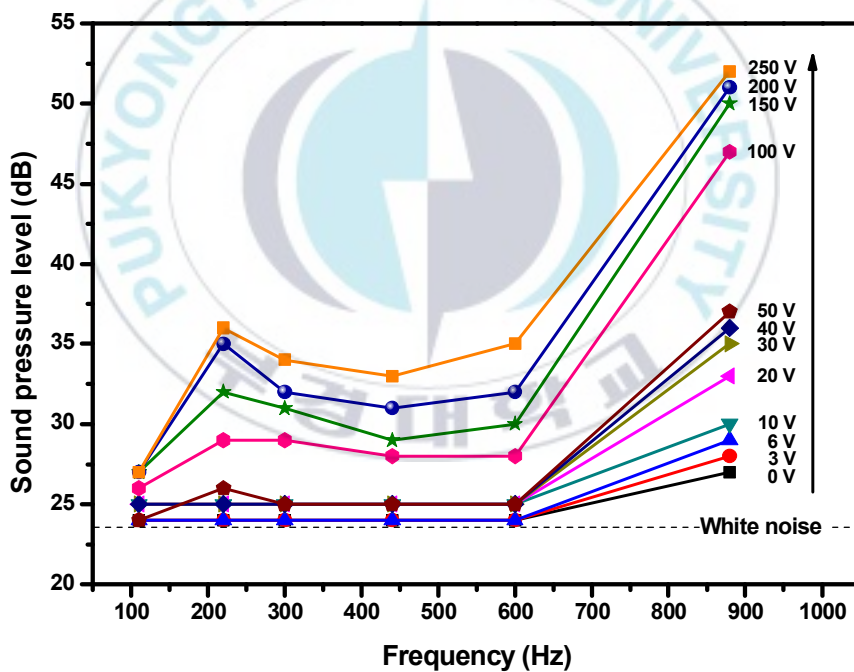


Figure 22. Frequency dependent SPL of acoustic EL device

As seen in figure 23 the SPL versus input voltage of the fabricated EL speaker shows a good linearity below the frequency of 600 Hz. This is due to the increase of the amplitude of the vibration of the piezoelectric ceramics according to the equation (2). Especially, the SPL of the EL speaker is by a factor 50 dB lower than the pure PZT speaker without the phosphor layer; the maximum SPL of EL speaker is 52 dB at the frequency of 880 Hz and the voltage of 250 V rms, and the maximum SPL of the pure PZT speaker reached about 100 dB at the same condition. This is the reason why the phosphor layer (phosphor powder in dispersed in organic binder) functions as a damping factor, in more details, the non-stiff organic binder. In addition, at the frequency of 880 Hz, the voltage response violates the linearity, i.e, saturation curve at the voltage of 100 V_{rms}. It can be explained by the breakdown of the phosphor layer at this voltage which is defined as the threshold voltage or turn-on voltage in EL device. This breakdown releases the storage charge of the PZT sheet so as to quench its piezoelectric effect.

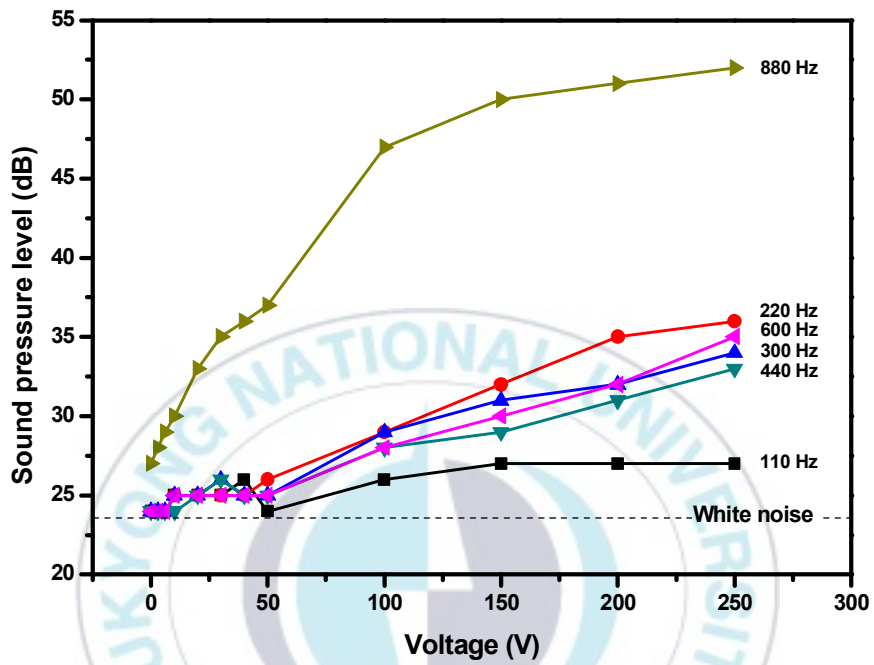
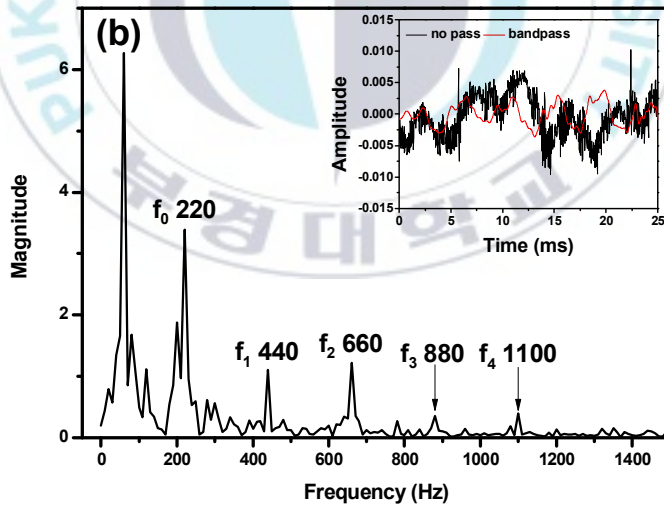
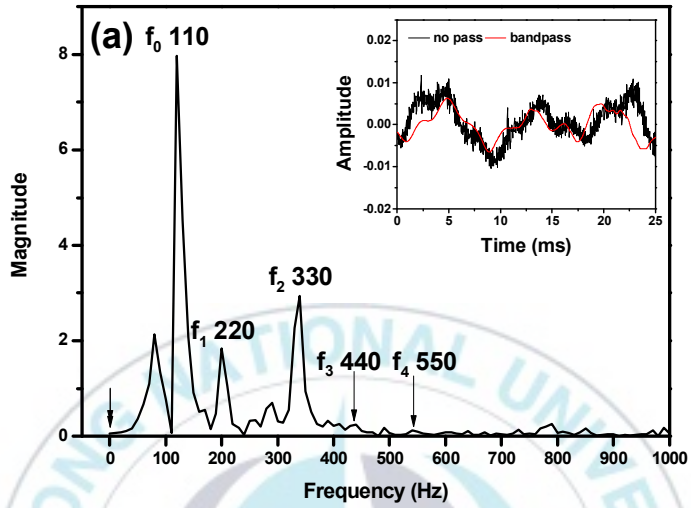


Figure 23. Voltage dependent SPL of acoustic EL device

4.5. Sound signals of acoustic EL device

Figure 24 shows the sound signal outputs of EL speaker in frequency domain. Each insets shows the sound signal outputs of EL speaker in time domain. The sound signal outputs in frequency domain are obtained by the fourier transform of the time-domain spectra. The various applied frequencies with a sin signal was applied to the EL speaker: $A_2 = 110\text{Hz}$ ("La" of second octave), $A_3 = 220\text{Hz}$ ("La" of third octave), $A_4 = 440\text{Hz}$ ("La" of fourth octave), $A_5 = 880\text{ Hz}$ ("La" of fifth octave) in scientific notation. All sound spectra shows first dominated magnitude at the same sound frequencies with the applied frequencies. The second strongest magnitude is observed at the triple of the applied frequencies. The signal at the double and quadruple frequencies are comparatively weak. These signals are attributed to second, third and fourth harmonic oscillations of the vibration plate. Finally the sum of all magnitudes over all harmonic frequencies are consistent with the SPL at 250 V and the applied frequencies, as shown in figure 22.



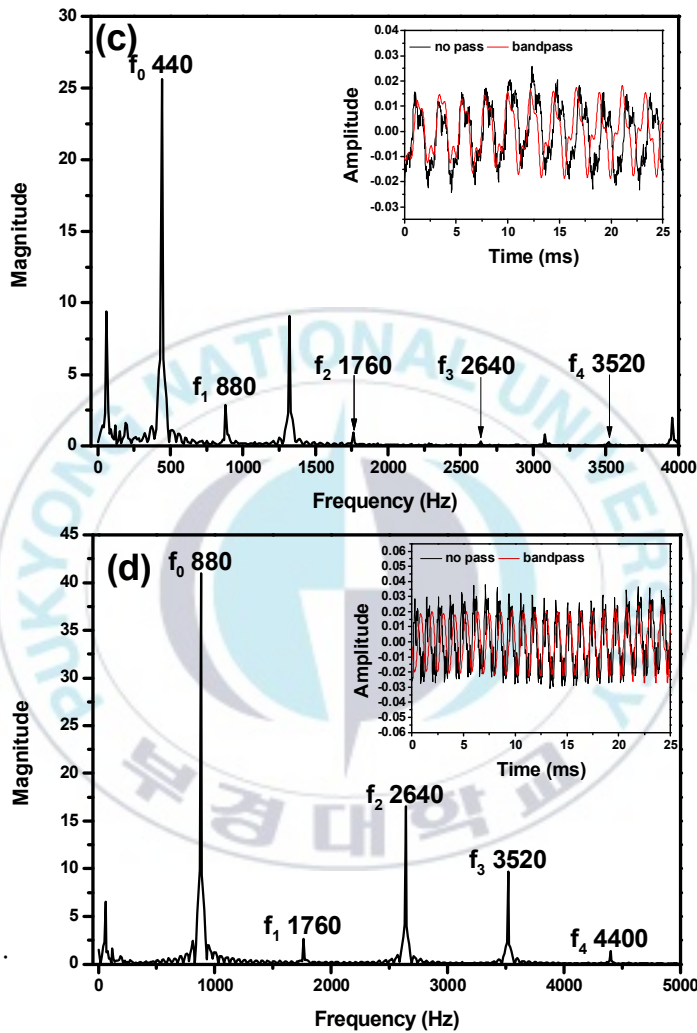


Figure 24. Sound signal outputs of EL speaker in frequency domain ; (a) $f_0=110$, (b) $f_0=220$, (c) $f_0=440$ and (d) $f_0=880$ Hz

V Conclusion

A novel electroluminescent (EL) device which emits sound as well as light, acoustic EL, has been achieved by using piezoelectric material as dielectric layer. This acoustic EL device consists of silver nanowires as top electrode, and ZnS:Mn²⁺ phosphor screen-printed on high piezoelectric material lead zirconate titanate (PZT) ceramic sheet. The ZnS:Mn²⁺ phosphor was synthesized by solid state reaction method and exhibits the photoluminescence peak at 581 nm and the electroluminescence peak at 583 nm. The silver nanowires on the top of ZnS:Mn²⁺ phosphor layer was spin-coated as a transparent top electrode due to their high transparency (85 %) and low sheet resistance (6 Ω/sq). The PZT ceramic sheet has high piezoelectric coefficient (d₃₃) as well as high dielectric constant (k). The high d₃₃ value (~ 400 pC/N) resulted in high sound pressure level up to 83 dB

at 100 V and 3,400 Hz. The high k value (~ 1650) caused to the high EL luminance up to about 2 cd/m^2 at 350 V and 400 Hz. The EL luminances was exponentially dependent on the applied voltage while the sound pressure levels was linearly dependent on the applied voltage, with the same threshold voltage of 50 V. The EL luminances was linearly increased and then saturated at the inverse of the decay time ($\sim 600 \text{ Hz}$) with increasing the applied frequency while the sound pressure levels showed the flat response below 600 Hz and then parabolic increase above 600 Hz. The temperature-dependent EL luminances were maximized at the temperature of $160 \text{ }^\circ\text{C}$, which is consistent with Curie temperature of the PZT sheet. Finally our EL device generated the lights from the phosphor as well as the sounds from PZT sheet with high thermal stability, so that it can be used as large-scale sheet-type EL speaker.

References

- [1] G. Destriu, J. Chem. Phys., 33, 587, 1936.
- [2] D. Kahng, Electroluminescence of rare earth and transition metal molecules in II VI compounds via impact excitation, Appl. Phys. Lett., 13, 210, 1968.
- [3] T. Inoguchi, M. Takeda, Y. Kakohara, Y. Nakata and M. Yoshida, in Digest, Int. Symp, Society for Information Display, 2, 84, 1974.
- [4] Y. Zhang, G. Gao, L. Helen, W. Chan, J. Dai, Y. Wang, and J. Hao, Piezo-Phototronic Effect-Induced Dual-Mode Light and Ultrasound Emissions from ZnS:Mn/PMN - PT Thin-Film Structures, Adv. Mater., 24, 1729, 2012.
- [5] T. Minami, T. Miyata, K. Kitamura, H. Nanto, and S. Takata, Sound Emitting Thin Film Electroluminescent Devices Using Piezoelectric Ceramics as Insulating Layer, Springer Proceedings in Physics, 38, 310, 1989.

- [6] C. Munasinghe, J. Heikenfeld, R. Dorey, R. Whatmore, Jeffrey P. Bender, John F. Wager and Andrew J. Steckl, High brightness ZnS and GaN electroluminescent devices using PZT thick dielectric layers, IEEE, Transaction On Electron Devices, 52, 194, 2005.
- [7] William M. Yen, S. Shionoya and H. Yamamoto, Phosphor handbook, CRC Press, New York, 2007
- [8] A. Mikami, K. Terada, K. Okibayashi, K. Tanada, M. Yoshida and S. J. Nakajima, J. Cryst. Growth, 110, 381, 1991
- [9] D. Theis, J. Lumin., 23, 191, 1981.
- [10] A. G. Fischer, J. Electrochem. Soc., 109, 1043, 1962.
- [11] A. G. Fischer, Electroluminescence in II-VI compounds in Luminescence of Inorganic Solids, Goldberg, P., Ed., Academic Press, New York, 1966.
- [12] E. W. Chase, R. T. Hoppelwhite, D. C. Krupka and D. J. Kalong, Appl. Phys., 40, 2512, 1969.
- [13] P. Zalm, Philips Res. Rep. 11, 353, 417, 1956.
- [14] F. Wang, Y. Jia, J. Wu, X. Zhao and H. Luo, Piezoelectric / electroluminescent Composites for Low Voltage input Flat-panel Display Devices, Appl. Phys. A, 90, 729, 2008.

- [15] X. L. Zhang, Z. X. Chen, L. E. Cross and W. A. Schulze, Dielectric and Piezoelectric Properties of Modified Lead Titanate Zirconate Ceramics from 4.2 to 300K, J. Mater. Sci., 18, 968, 1983.
- [16] A. Vecht, N. J. Werring, P. J. F. Smith, Brit. J. Appl. Phys, 1, 134, 1968.
- [17] L. E. Shea, R. K. Datta , J. Brown Jr., J. Electrochem. Soc. 141, 2198, 1994.
- [18] P. Zalm, G. Diemer, H. A. Klasens, Philips Res. Rep. 10, 205. 1955.
- [19] Hye Jin K, Woo Seok Y and Kwang soo N, Improvement of low-frequency characteristics of piezoelectric speakers based on acoustic diaphragms, IEEE Transactions on Ultrasonics, Ferroelectrics and Frequency Control, 59. 2027, 2012.
- [20] T. Yanagisawa and N. Koike, Cancellation of both Phase Mismatch and Position Errors with Rotating Microphones in Sound Intensity Measurement., J. Sound Vib., 113, 117, 1987.

ZnS:Mn/PZT 기반의 음향 출력 전계발광 소자

이 운 호

부경대학교 과학기술융합전문대학원 LED융합공학전공

요약

본 연구에서는 전계발광 소자의 유전층을 압전 특성을 지닌 물질을 사용함으로써 전계발광뿐 아니라 음향 출력이 가능한 소자를 구현했다. 음향 출력 전계발광 소자는 고압전 특성을 지닌 PZT 세라믹 판에 ZnS:Mn²⁺ 형광체를 스크린 인쇄한 후 은나노 와이어 상부 투명전극으로 구성되어 있다. ZnS:Mn²⁺ 형광체는 고상반응법으로 합성했다. PZT 세라믹 판은 높은 압전 효율 특성 (d_{33})과 동시에 높은 유전 상수 (k)를 가진다. ~ 400 pC/N의 d_{33} 값을 가지는 소자의 음압 수치는 100 V 및 3,400 Hz를 인가하였을 때 83 dB을 가진다. ~ 1650 의 유전 상수를 가지는 소자는 350 V 및 400 Hz를 인가하였을 때 2 cd/m²의 휘도값을 가진다. 소자의 전계발광은 인가 전압에 대하여 기하급수적인 의존도를 가지며 음압 수치는 인가 전압에 대하여 선형적인 의존도를 가진다. 발광 및 음압의 문턱 전압은 50 V로 동일하다. 전계발광 휘도값은 발광의 감쇠 시간의 역수(~ 600 Hz)에서 포화되고, 소자의 음압 수치는 600 Hz 이하에서 평평한 반응을 보이다가 600 Hz 이상일 때

포물선형으로 증가한다. 전계발광의 온도의존도는 160 °C에서 최고치를 나타내며, PZT의 큐리 온도와 일치하는 현상을 보였다.

keyword : 전계발광소자, 압전소자, ZnS:Mn^{2+} 형광체,
티탄산 지르콘산 연 (PZT)

